Fabrication and magnetocrystalline anisotropy of NiCo(002) films*

Fan Wei-Jia(樊维佳), Ma Li(马 丽), Shi Zhong(时 钟), and Zhou Shi-Ming(周仕明)†

Shanghai Key Laboratory of Special Artificial Microstructure and Pohl Institute of Solid State Physics and School of Physics Science and Engineering, Tongji University, Shanghai 200092, China

(Received 26 July 2014; revised manuscript received 14 October 2014; published online 19 January 2015)

A series of 30-nm-thick epitaxial Ni_xCo_{1-x} (002) alloy films are fabricated by DC magnetron sputtering. MgO (002) and $SrTiO_3$ (002) single substrates are used for $x > 0.5$ and $x < 0.5$, respectively. The magnetocrystalline anisotropy of Ni_xCo_{1-x} (002) alloy films is studied in the entire composition region for $0 \leq x \leq 1.0$. When x decreases, the cubic magnetic anisotropy constant K_1 changes sign from negative to positive at $x = 0.96$ and becomes negative again at $x = 0.79$. It becomes more negative as x decreases from 0.79 to 0. The uniaxial anisotropy K_u is smaller than the K_1 by a factor of two orders.

Keywords: face centered cubic CoNi alloy, magnetocrystalline anisotropy

PACS: 75.70.–i, 75.30.Gw, 75.50.Cc **DOI:** 10.1088/1674-1056/24/3/037507

1. Introduction

Magnetic anisotropy of magnetic materials has always been a subject of interest in condensed matter physics. As is well known, magnetocrystalline anisotropy (MCA) arises from both the spin–orbit coupling (SOC) and the exchange split.[1] Within the frame of the perturbation theory, the magnetic anisotropy constant may be proportional to the SOC strength ξ^2 and ξ^4 for uniaxial anisotropy and cubic anisotropy, respectively.[1] For L1(0) FePtPd ternary alloys,[2,3] for example, the perpendicular magnetic anisotropy is found to be proportional to $\xi^{1.5}$. More remarkably, the MCA of transition metallic alloys is also found to strongly depend on the numbers of 3d electrons in the valence band.[4–6] For bulk centered cubic (BCC) NiFe alloys, the cubic magnetic anisotropy constant K_1 approaches zero near $Ni_{0.8}Fe_{0.2}$ due to the band-filling effect of 3d band, although K_1 is positive for BCC Ni and Fe.[10]

The MCA of 3d magnetic alloys has been studied extensively.[7–12] For bulk Ni-rich NiFe alloys with face centered cubic (FCC) structure, the sign change is located near the composition of $Ni_{0.8}Fe_{0.2}$.[8] In contrast, the composition dependence of the MCA of bulk Ni_xCo_{1-x} (=NiCo) is rather complicated,[7,9] compared with that of NiFe alloys. For the bulk Ni-rich NiCo alloys with FCC structure, the K_1 changes the sign from negative to positive at 4 at.% Co and then once again turns negative near 20 at.% Co.[7] Furthermore, the MCA of FCC Co-rich NiCo alloys has seldom been studied despite its crucial importance. This is partly because bulk Co-rich NiCo alloys at the equilibrium state are of hexagonal close-packed (HCP) structure instead of the FCC structure. Fortunately, the epitaxial FCC Co films and Co-rich NiCo films have very recently been fabricated on single crystal substrates by molecular beam epitaxy or magnetron sputtering.[13] Therefore, we are allowed to study the MCA of Ni_xCo_{1-x} alloys within the entire composition region. In this work, we have successfully fabricated a series of epitaxial FCC Ni_xCo_{1-x} (002) alloy films with $0 \leq x \leq 1.0$, and then studied the MCA by the magnetic torque technique. It is found that the K_1 of the Ni-rich Ni_xCo_{1-x} (002) films exhibits a similar variation trend for Ni-rich NiCo bulk alloys. For Co-rich NiCo epitaxial films, the K_1 is negative and its magnitude increases with decreasing x.

2. Experiments and results

Ni_xCo_{1-x} thin films were fabricated on MgO (002) single crystalline substrates for $x > 0.5$ and on $SrTiO_3$ (002) single crystalline substrates for $x < 0.5$ in a high vacuum DC magnetron sputtering system. Here, $SrTiO_3$ substrates favor fabrication of the epitaxial Co-rich NiCo films.[14] The samples were deposited from NiCo alloy targets, which were formed by adding Co/Ni small pieces on Ni/Co targets. The base pressure was 1×10^{-5} Pa and the working Ar pressure was 0.35 Pa. The deposition rate of Ni_xCo_{1-x} films was about 0.1 nm/s. The MgO and $SrTiO_3$ substrates were first annealed at 500 °C and 650 °C for one hour to annihilate possible contamination on the surface, respectively. The temperatures of MgO and $SrTiO_3$ substrates were then kept at 300 °C and 500 °C during deposition of Ni-rich and Co-rich NiCo films, respectively, and post-annealing was performed at the same temperature for two hours. The microstructure and thickness of films were characterized by x-ray diffraction (XRD) and x-ray reflectivity (XRR) by a Bruker D8 diffractometer with 5-axis configuration and Cu Kα ($\lambda = 0.1542$ nm), respectively. The epitaxial

*Project supported by the National Natural Science Foundation of China (Grant Nos. 11374227, 51331004, 51171129, and 51201114) and the Shanghai Science and Technology Committee, China (Grant Nos. 0252nm004, 13XD1403700, and 13520722700).

†Corresponding author. E-mail: shiming@tongji.edu.cn

© 2015 Chinese Physical Society and IOP Publishing Ltd

growth was proven by the x-ray pole figures. The alloy composition was characterized by energy dispersive x-ray spectroscopy (EDX) in combination with scanning electronic microscopy (SEM). In-plane magnetization hysteresis loops and magnetic torque curves were measured by a vector vibrating sample magnetometer (VVSM) of Lakeshore 7407. Components of the magnetization parallel and perpendicular to the external magnetic field H, M_x, and M_y, were measured simultaneously. In the presence of an in-plane H, M_x, and M_y were both parallel to the film plane. Here, the curve of M_x versus H corresponds to the conventional magnetization hysteresis loop. In magnetic torque measurements, M_y was measured as a function of the orientation of the sample under a fixed H and the magnetic torque, i.e., the product of the M_y and H, was obtained. All of the measurements were performed at room temperature.

The film thickness characterized by XRR is 30±1.0 nm. Figures 1(a) and 1(b) present the typical XRD spectra of Co-rich and Ni-rich NiCo films, respectively. For Co-rich NiCo films on $SrTiO_3$ (002) substrates in Fig. 1(a), two peaks near $2\theta = 46°$ and 52°, correspond to $SrTiO_3$ (002) and Ni_xCo_{1-x} (002) orientations,[13] respectively. For Ni-rich NiCo films on MgO substrates in Fig. 1(b), two peaks are found at $2\theta = 42°$ and 52°, which refer to MgO (002) and Ni_xCo_{1-x} (002) orientations, respectively. The XRD peak of the Ni_xCo_{1-x}(002) almost does not shift with x and the lattice constant of Ni_xCo_{1-x} films along the film normal direction is about 0.3524 nm for all samples, which is close to their bulk value.[15] This happens because the strain of epitaxial films is relaxed when the film thickness is larger than a critical value. It is noted that there is no diffraction peak near $2\theta = 75°$ for HCP $(11\bar{2}0)$ Co.[13] In order to prove the epitaxial growth of Ni_xCo_{1-x} films, ϕ scanning was performed for Ni_xCo_{1-x} films and substrates. Figure 1(c) shows that the Co film and $SrTiO_3$ substrate have the same four-fold symmetry, where $2\theta = 44.36°$ for the Co film and $2\theta = 39.98°$ for the $SrTiO_3$ substrate. In experiments, it is found that $SrTiO_3$(002) substrates are more suitable for the epitaxial growth of the Co-rich NiCo films, compared with the MgO(002).[14] With MgO(002) substrates, Co-rich NiCo films are of both FCC and HCP phases at the same fabrication condition. It is expected that FCC Ni_xCo_{1-x} epitaxial films on $SrTiO_3$ substrates have a smaller strain when compared with the MgO(002) ones. In other words, the Ni-rich and Co-rich NiCo(002) films are epitaxially well grown on the MgO and $SrTiO_3$ substrates.

Figures 2(a)–2(f) show typical hysteresis loops of Co film and $Ni_{0.8}Co_{0.2}$ film ($x = 0.8$) along [200], $[\sqrt{3}10]$, and [220], respectively. It can be seen that for the Co film, the hysteresis loop along [220] is more squared than those at other orientations, and thus the easy axis is aligned along the [220] orientation. In contrast, the easy axis for $x = 0.80$ is aligned along the [200]. Therefore, the K_1 is negative for $x = 0$ and positive for $x = 0.80$, as further proved below. Moreover, the coercivity of $x = 0.8$ is much smaller than that of $x = 0$. As shown in Fig. 3, the angular dependencies of the remanent ratio and the coercivity for the Ni films clearly illustrate the four-fold symmetry of the Ni films, which is in agreement with the XRD results.

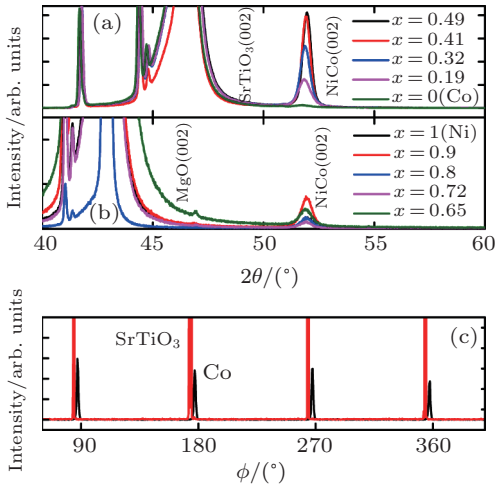


Fig. 1. (color online) XRD spectra of Co-rich NiCo films on $SrTiO_3$ substrates (a) and Ni-rich NiCo films on MgO substrates (b), ϕ scanning at $2\theta = 44.36°$ for the Co film and 39.98° for the $SrTiO_3$ substrate (c).

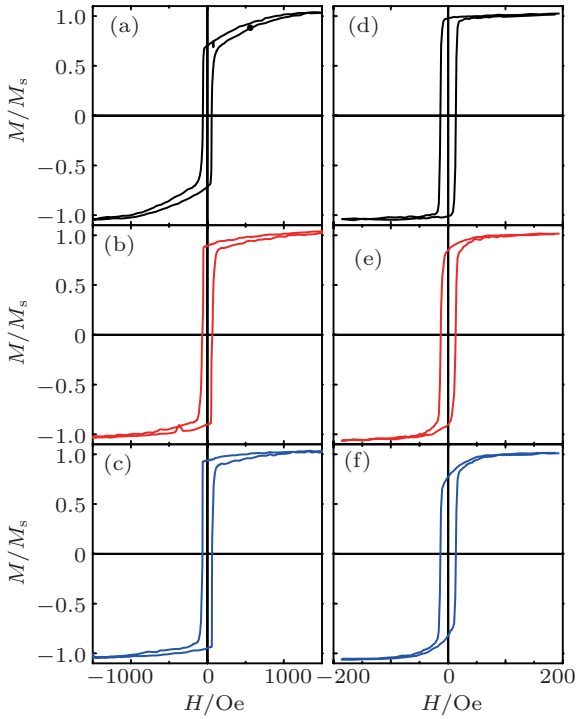


Fig. 2. (color online) Typical in-plane hysteresis loops of the Co (left column) and $Ni_{80}Co_{20}$ (right column) films for H along the [200] ((a) and (d)), $[\sqrt{3}10]$ ((b) and (e)), [220] ((c) and (f)).

To get the K_1 and K_u, magnetic torque curves were measured for the Ni_xCo_{1-x} films. Figure 4(a) shows typical torque curves for Co, $Ni_{0.8}Co_{0.2}$, and Ni films. All three samples have four-fold symmetry. The magnetic torque changes similarly for Co and Ni films, whereas it varies in an opposite way

for the $Ni_{0.8}Co_{0.2}$ films. Moreover, the Co film has the largest magnitude in the torque curve and the $Ni_{0.8}Co_{0.2}$ film has the smallest one, indicating the effect of the alloy composition on the magnetic anisotropy constants.

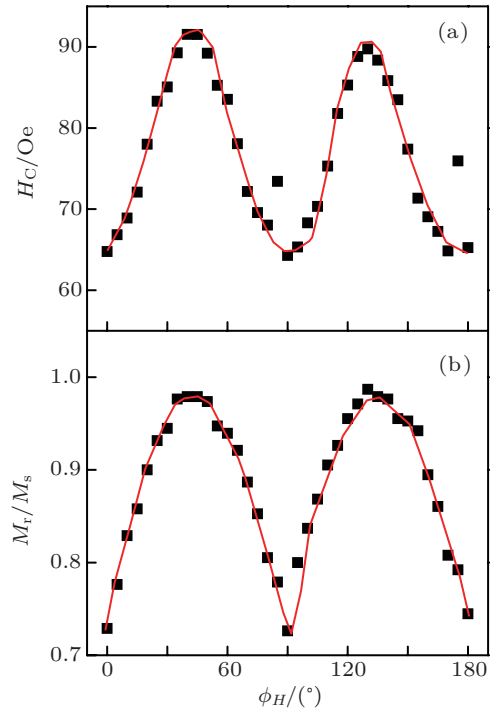


Fig. 3. (color online) For the Ni film, the coercivity (a) and remanent ratio (b) as a function of the orientation of the external magnetic field. Solid lines serve a guide to the eye. Here, $\phi_H = 0$ for H along the [200].

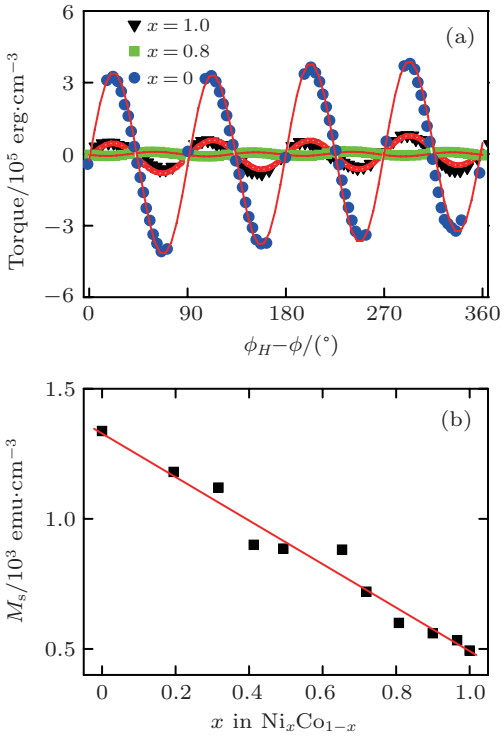


Fig. 4. (color online) (a) Torque as a function of the angle difference between the external magnetic field and the magnetization vector, and (b) the spontaneous magnetization M_s versus the x. The solid lines refer to the fitted results in panel (a) and serve a guide to the eye in panel (b). In panel (a), $H = 200$ Oe for $x = 0.80$, and $H = 1.0$ kOe for $x = 0$ and 1.0.

The magnetic torque curves can be fitted as follows. The free energy of the Ni_xCo_{1-x} films includes the MCA, uniaxial anisotropy, and the Zeeman energy, and it reads as follows:

$$E = K_1 \sin^2(\phi)\cos^2(\phi) + K_u \sin^2(\phi) - MH\cos(\phi - \phi_H), \quad (1)$$

where ϕ and ϕ_H are the angles of the magnetization vector and the external magnetic field with respect to [200]. At a specific orientation of the external magnetic field, the equilibrium angular position can be obtained from the equation $\partial E/\partial\phi = 0$. Accordingly, the magnetic torque can be calculated by the following equation, $L = M_s H \sin(\phi - \phi_H)$. Since the magnetic torque curves can be fitted very well in Fig. 4(a) the K_1 and K_u can be deduced. For the Co (002) films, the $K_1 = -7.6 \times 10^5$ erg/cm^3. In the above fitting process, the saturation magnetization M_s at room temperature is shown in Fig. 4(b). The M_s decreases from 1330 emu/cm^3 for Co to 493 emu/cm^3 for Ni, which is in agreement with the Slater–Pauling curve.[16] The value of M_s for the FCC Co film is also close to the reported results from other research groups.[17–21]

Figure 5(a) shows that with increasing x, K_1 increases from negative to positive values at $x = 0.79$, and then turns negative again. In the region from $x = 0.79$ to 1.0, the values of the K_1 for the present films are close to other reported results.[7] For $0.35 < x < 0.7$, however, the K_1 for the present Ni_xCo_{1-x} films is larger than the results given by other research groups.[17,22] It is noted that the K_1 of the present Ni film is smaller than that of 5.6×10^5 erg/cm^3 for bulk FCC Ni.[9] The discrepancy of the K_1 may arise from the different lattice constants.[18,19,23–25] For the present epitaxial Ni_xCo_{1-x} films, the lattice constant along the film normal direction is 0.352 nm for all x whereas for bulk FCC-NiCo crystals, the lattice constant changes from 0.354 to 0.352 nm for x from 0 to 1.0.[15] For the present epitaxial Co films, the lattice constant c is reduced by 0.45% when compared with the bulk FCC Co.

For the present Ni_xCo_{1-x} films, the non-monotonic change of the K_1 is in agreement with the theoretical prediction.[11,26] The *ab initio* calculations show that the orbital moment and the magnetostriction coefficient of NiCo alloys change non-monotonically with the alloy composition due to the band-filling effect.[26] The effective SOC strength and the MCA are expected to have similar variation trends. Therefore, the non-monotonic variation of the K_1 in Fig. 5(a) can be explained in terms of the band-filling effect. It is noted that in the Ni_xCo_{1-x} (002) films, the second order of the MCA K_2 cannot be obtained from the magnetic torque measurements. As shown in Fig. 5(b), the K_u is smaller than the K_1 by a factor of two orders and the data are much more scattered.

It is interesting to analyze the composition depedence of the in-plane coercivity along the easy axis. Figure 5(c) shows that the in-plane coercivity has a minimum near $x = 0.90$ because the magnetization reversal mechanism of Ni_xCo_{1-x} films is mainly determined by the MCA and the Ni_xCo_{1-x} (002) films near $x = 0.9$ are soft magnetic materials due to small K_1. Moreover, for most of the epitaxial Ni_xCo_{1-x} (002) films the coercivity is smaller than the anisotropic field, indicating the multidomain magnetization reversal process. For example, the coercivity and the anisotropic field are 76 and 123 Oe for the Co film, respectively. Finally, the interfacial morphology should also be considered. For example, Lukaszew *et al.* have found the coercivity of the Ni films on the MgO substrate is 200 Oe,[27] which is much larger than that (90 Oe) of the present Ni film, this was attributed to the exchange bias induced by an ultrathin NiO layer at the Ni/MgO interface. For the present Ni film, a clean Ni/MgO interface is therefore obtained without any NiO ultrathin layer at the interface.[28]

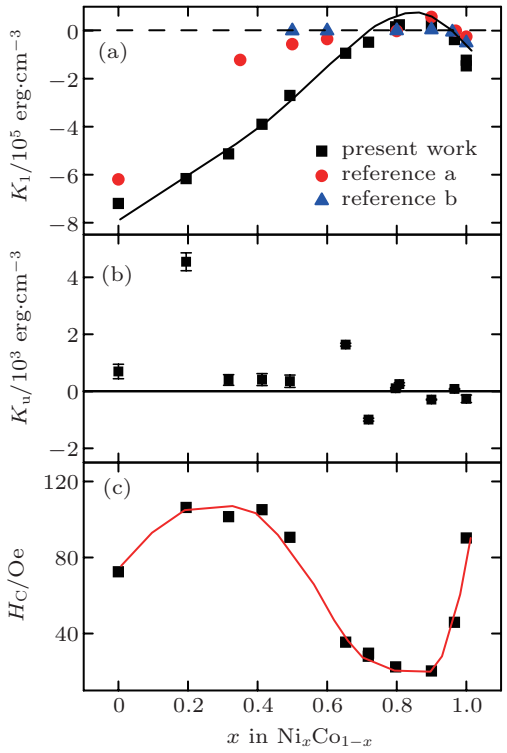


Fig. 5. (color online) K_1 (a), K_u (b), and the coercivity H_C along the film plane (c) at room temperature as a function of x. In comparison, data from Refs. [7] (reference a, red solid circles) and [9] (reference b, blue uptriangle) are given in panel (a). The solid lines serve a guide to the eye.

3. Summary

In summary, we have fabricated 30-nm-thick epitaxial Ni_xCo_{1-x} films on MgO(002) substrates for $x > 0.5$ and on $SiTiO_3$ substrates for $x < 0.5$. The K_1 increases from negative to positive with a crossover near $x = 0.79$ when x changes from 0 to 0.90. As x further increases, the K_1 decreases from positive to negative with a crossover near $x = 0.95$. For the Ni_xCo_{1-x} films $x > 0.35$, the composition dependence of the K_1 reproduces the results of bulk NiCo alloys. The in-plane coercivity also changes non-monotonically with x, exhibiting a minimal value near $x = 0.90$. These results will be helpful to understand the MCA of 3d transition metals and alloys.

References

[1] Bruno P 1993 *Physical Origins and Theoretical Models of Magnetic Anisotropy* (Ferienkurse des Forschungszentrums Jülich, Jülich)
[2] Ma X, He P, Ma L, Guo G Y, Zhao H B, Zhou S M and Lüpke G 2014 *Appl. Phys. Lett.* **104** 192402
[3] He P, Ma X, Zhang J W, Zhao H B, Lüpke G, Shi Z and Zhou S M 2013 *Phys. Rev. Lett.* **110** 077203
[4] Daalderop G H O, Kelly P J and Schuurmans M F H 1991 *Phys. Rev. B* **44** 12054
[5] Sakuma A, Manabe Y and Kota Y 2013 *J. Phys. Soc. Jpn.* **82** 073704
[6] Schneider G 1999 Ph. D Thesis (Oregon State University)
[7] Shih J W 1936 *Phys. Rev.* **50** 376
[8] Bozorth R M and Walker J G 1953 *Phys. Rev.* **89** 624
[9] Hall R C 1959 *J. Appl. Phys.* **30** 816
[10] Yin L F, Wei D H, Lei N, Zhou L H, Tian C S, Dong G S, Jin X F, Guo L P, Jia Q J and Wu R Q 2006 *Phys. Rev. Lett.* **97** 067203
[11] Zhang S, Pang H, Fang Y and Li F S 2010 *Chin. Phys. B* **19** 127102
[12] Li R W, Liu Y W and Zhan Q F 2013 *Chin. Phys. B* **22** 127502
[13] Ohtake M, Nukaga Y, Sato Y, Kirino F and Futamoto M 2009 *J. Appl. Phys.* **106** 123921
[14] Sato Y, Nishiyama T, Ohtake M, Kirino F and Futamoto M 2010 *IEEE Trans.* **46** 349
[15] Pearson W B 1958 *A Handbook of Lattice Spacings and Structures of Metals and Alloys* (London: Pergamon Press)
[16] Chikazum S 1997 *Physics of Ferromagnetism* (Oxford: Clarendon Process)
[17] Wolf J A, Krebs J J and Prim G A 1994 *Appl. Phys. Lett.* **65** 1057
[18] Oepen H P, Berming M, Ibach H, Schneider C M and Kirschner J 1990 *J. Magn. Magn. Mater.* **86** L137
[19] Chang C A 1992 *J. Magn. Magn. Mater.* **109** 243
[20] Wu R and Freeman A J 1992 *J. Magn. Magn. Mater.* **116** 202
[21] Li C, Freeman A J and Fu C L 1988 *J. Magn. Magn. Mater.* **75** 53
[22] Rodbell D S 1962 *J. Phys. Soc. Jpn.* **17** B-1 313
[23] Kerkmann D, Wolf J A, Pescia D, Woike Th and Grünberg P 1989 *Solid State Commun.* **72** 963
[24] Kief M T, Mankey G J and Willis R F 1991 *J. Appl. Phys.* **69** 5000
[25] Inaba N, Uesaka Y and Futamoto M 2000 *IEEE Trans. Magn.* **36** 54
[26] James P, Eriksson O, Hjortstam O, Johansson B and Nordström L 2000 *Appl. Phys. Lett.* **76** 915
[27] Lukaszew R A, Mitra M, Zhang Z and Yeadon M 2005 *Eur. Phys. J. B* **45** 181
[28] Fan Y, Smith K J, Lupke G, Hanbicki A T, Goswami R, Li C H, Zhao H B and Jonker B T 2013 *Nat. Nanotechnol.* **8** 438